

Short Communication

Effect of Lateral Dimension of Natural Graphite on Fabrication of Three-Dimensional Graphene Aerogels for High-performance Li-metal anodes

Huan Zhang^{1,2}, Xinxiu Yan³, Yingjun Qiao^{1,2}, Huimin Shang^{1,2}, Meiling Huang¹, Xuemei Zhou¹, Hanxiao Zhou^{1,2}, Tianhui Li^{1,2}, Jingjing Gao^{1,2}, Wenjing Liu^{1,2}, Meizhen Qu¹, Gongchang Peng^{1,*}, Xue Li^{4,*}

¹ Chengdu Institute of Organic Chemistry, Chinese Academy of Sciences, Chengdu, Sichuan 610041, China

² University of Chinese Academy of Sciences, Beijing 100049, China

³ School of Chemistry and Environment, Southwest Minzu University, Chengdu 610041, China

⁴ National and Local Joint Engineering Laboratory for Lithium-ion Batteries and Materials Preparation Technology, Faculty of Metallurgical and Energy Engineering, Kunming University of Science and Technology, Kunming 650093, PR China

*E-mail: pgc0102@cioc.ac.cn (Gongchang Peng), 438616074@qq.com (Xue Li))

Received: 1 December 2020 / Accepted: 25 January 2021 / Published: 28 February 2021

Lithium metal, regarded as one of the most potential anodes for future battery systems, has attracted much attention for a long time. Nonetheless, uncontrollable Li dendrites growth and almost infinite volume change hinder the reliable implementation of lithium anode. Three-Dimensional graphene aerogel is an ideal lithium metal host material because of its abundant porous structure and large surface area, which can relieve the volume change, as well as reduce the effective current density. The lateral dimension of raw material natural graphite will affect the morphology and hierarchical structures of graphene aerogels, thereby affecting the electrochemical properties as a lithium host material. A series of graphene aerogels were prepared from natural graphite with different lateral dimensions (3.4 μm 、11 μm 、44 μm 、178 μm) for Li host material. The GA-11/Li composite anode exhibits the best electrochemical performance. The symmetrical cell with GA-11/Li electrode shows stable cycling for 600 h at 2 mA cm^{-2} for 2 mAh cm^{-2} . Surprisingly, the Li-S full cell with GA-11/Li anode delivers a high initial specific discharge capacity of 9.38 mAh cm^{-2} and stable cycle stability.

Keywords: Lithium metal anode, graphene aerogel, different lateral dimensions, cycling stability

1. INTRODUCTION

Owing to its outstanding features, especially the far higher theoretical gravimetric capacity (3860 mAh g^{-1}) and the lowest standard electrode potential (-3.04 V), lithium metal is regarded as an

ideal anode for next generation batteries [1, 2]. Nevertheless, several inevitable problems of lithium metal anode limit its further applications, such as uncontrollable growth of Li dendrites, limitless volume expansion during dissolution/deposition process of Li, and insecure solid electrolyte interface (SEI) film [3, 4]. These problems cause poor cycling life of lithium anode, low Coulombic efficiency (CE), or even serious safety problems. In order to solve these issues, massive efforts have been made and many solutions have been studied, including adding various electrolyte additives (LiNO_3 , Cs^+ , Li_2S_6 , LiF , FEC , $\text{Cu}(\text{CH}_3\text{COO})_2$, etc.) or optimizing the electrolyte to maintain the stability of the SEI layer and prevent the Li dendrites growth [5-7], introducing artificial SEI films to regulate ion distribution, tailor the composition of the SEI, inhibit the penetration of Li dendrites and improve CE [8, 9]. Although these strategies can mitigate SEI collapse and prevent the formation of Li dendrite in some degree, the infinite relative dimension variation caused by the 'hostless' cannot be relieved during cycling.

Many stable hosts with abundant porous structures and large specific surfaces have been considered as a promising choice to adapt the dimension changes and reduce the growth rate of Li dendrite. Multifarious rational designed three-dimensional (3D) porous carbon materials are ideal host candidates, such as layered reduced graphene film [10], 3D nanoporous nitrogen-doped graphene [11], 3D carbon fiber network [12], 3D carbon nanotube matrix and 3D fluorine-doped graphene because of their unique advantages [13, 14]. 3D graphene aerogel, with its super electrical conductivity, huge specific surface area, and feathery density ($<10 \text{ mg cm}^{-3}$), is a superior carbon material that able to be a Li metal anode carrier. Lu et al. [15] fabricated a series of graphene aerogel with different porosity and prepared the GA/Li composite electrode by an electrochemical deposition method. The electrode has a high lithium/carbon mass ratio (5:1) and long cycle stability. Zhao et al. [16] reported a well-designed graphene aerogel/Ag composite fabricated by a one-step hydrothermal method as a lithium host material. In the GA/Ag structure, Ag nanoparticles were homogeneously embedded in the graphene layers, which enhanced the lithiophilicity of the graphene matrix. Even in carbonate-based electrolytes, the GA/Ag electrode exhibited high coulombic efficiency (CE) and good cycle stability. The high-temperature thermal melting is a convenient and effective procedure for filling lithium into the host matrices of the carbon materials [17]. The degree of oxidation and the lateral dimension of graphene oxidation (GO) directly affect the pore structure and morphology of the prepared graphene aerogel [18, 19]. Graphene oxide is obtained by the oxidation of natural graphite. The lateral dimension of the natural graphite determines the size and oxidation degree of the GO. The morphology and hierarchical pore structures of graphene aerogel are crucial for determining the electrochemical property of the lithium metal composite anode [20]. Therefore, the study of graphene aerogels prepared from different lateral dimensions of natural graphite as optimized lithium matrix materials has great advantages. It is necessary to analyze the distinction in electrochemical performance of the electrodes, which are composite lithium with a series of graphene aerogels prepared from different sizes of natural graphite.

In this work, we fabricated a series of graphene aerogels via a hydrothermal method, followed by freeze-drying and high-temperature calcination processes. The raw precursors of the graphene aerogels are natural graphite with different lateral dimensions (3.4 μm 、11 μm 、44 μm 、178 μm). Different GA/Li composite anodes were prepared by high-temperature thermal melting, and their electrochemical performances were compared as well. The experimental results indicate that all

graphene aerogels prepared from natural graphite with different layer dimensions have ultra-low mass density, abundant holes and a large specific area, which provide space to migrate the volumetric expansion during Li plating/stripping cycles and decrease the partial current density. The morphology and specific surface area of the four graphene aerogels are different, GA-11 has the largest specific surface area (185.96 m²/g). Among all the GA/Li composite anodes, GA-11 reinforced Li anode shows the best electrochemical performance. The symmetrical GA-11/Li | GA-11/Li cell shows remarkable cycling stability for 600 h at 2 mA cm⁻² for 2 mAh cm⁻². Furthermore, the full cell coupling with sulfur was assembled, the GA-11/Li | S full cell still presents good cycling stability although the sulfur loading is up to 9.4 mg cm⁻².

2. EXPERIMENT

2.1 Preparation of graphene aerogel (GA)

The portion of graphene aerogel (GA) samples were prepared using graphene oxide (GO) as precursors, which were synthesized by the oxidation of natural graphite with different lateral dimensions (3.4 μm, 11 μm, 44 μm, 178 μm) using a modified Hummers' method. The graphene aerogels were fabricated by hydrothermal approach, after freeze-drying, the samples were heat-treated as reported previously [19]. 15 mL of uniform GO aqueous dispersoid (4 mg mL⁻¹) and 80 μL of ethylenediamine (EDA, C₂H₄(NH₂)₂) were mixed and the mixture was ultrasonically dispersed for 20 mins. Successively, this mixture was stucked in a 25 mL sealed Teflon-lined autoclave and then maintained at 120 °C for 16 h. The formed graphene hydrogels were washed repeatedly with ethanol/deionized water (12:88 v/v) followed by freeze-dried for 2 days. Finally, the GA samples were obtained through thermal reduction at 800°C for 12 h under Ar atmosphere.

2.2 Synthesis of graphene aerogel-Li (GA/Li) anodes

The as-obtained graphene aerogel samples were transferred to a glove box full of argon atmosphere. A certain amount of GA (the mass ratio of graphene and Li is 1:9) was then put into the melted Li, which melted in a hot pan at 200 °C, and the mixture was stirred vigorously for one hour. The molten Li was infused into the pores of the graphene aerogel with the color of the mixture changed from black to silver, then the slurry was pasted on a commercial copper screen and naturally cooled down to room temperature. Before being assembled into cells, the GA/Li electrodes were pressed to obtain smooth surfaces.

2.3 Material Characterization

The scanning electron microscopy (SEM, Acceleration voltage: 20 kV, FEI Sirion-200 Netherlands) was employed to characterize the microstructures and size of the prepared GA and Li composite anodes. X-Ray Diffraction (XRD) patterns were recorded on an X'pert MPD DY1219

instrument. The Brunauer-Emmett-Teller (BET) specific surface areas of the graphene aerogels were measured on a Micromeritics' system (ASAP 2020, USA). X-ray photoelectron spectroscopy (XPS, PHI 5600 Physical Electronics) measurements were achieved using Al ($K\alpha$) monochromatic beam.

2.4 Electrochemical measurements

The GA/Li electrodes were cropped to wafers with a diameter of 10 mm, the Li anodes were tailored in the same way. The cells were made by using CR2032 coin shell under inert atmosphere, the working and counter electrodes used here are both GA/Li electrodes in symmetric cells. Full-cell coins were assembled using S electrode as cathodes, and its preparation process was adopted from previous report, the quality loading of sulfur in the cathode was 9.4 mg cm^{-2} . GA/Li foils (diameter of 16 mm) were used as the counter electrode, and Celgard 2400 was served as the separator. The electrolyte comprised 1 M LiTFSI and 2 wt % LiNO_3 addition in 1, 3-dioxolane (DOL) and 1,2-dimethoxyethane (DME) (1:1 in volume), the electrolyte/sulfur ratios for the full-cell coins was $12 \text{ }\mu\text{L mg}^{-1}$. Galvanostatic charge/discharge measurements were measured in 1.7-2.8 V on a multichannel battery test system (Land CT2001a, Wu Han, China).

3. RESULTS AND DISCUSSION

The SEM images of the graphene aerogels are shown in Figure 1, which were obtained by a self-assembly hydrothermal reduction process from graphene oxide [19], which was synthesized by the oxidation of graphite with different layer sizes. After reduction, the graphene oxide has formed a three-dimensional structure with lamellar folds and cross-linked holes. Besides, there are distinctions among the morphologies of graphene aerogels prepared from different sizes of graphite. It can be seen that as the lateral dimensions of natural graphite increase, the transparency of the graphene aerogel lamella increases. Among them, the lamellas of GA-3.4 made of $3.4 \text{ }\mu\text{m}$ graphite are stacked together, and these lamellas are thick and have no obvious folds. The three-dimensional structure of graphene aerogel prepared from $11 \text{ }\mu\text{m}$ graphite (GA-11) has the smallest, most regular pore size and obvious folds. Compared to other reported carbon host materials [12, 13], the graphene aerogel-11 presents a unique hierarchical porous structure with uniform pore size, which is beneficial to moderate the huge volume expansion in lithium plating/stripping cycles.

Figure 2 is the N_2 adsorption-desorption isotherms of four prepared graphene aerogels. When the relative pressure is greater than 0.2, a small hysteresis loop is observed in all four curves, which indicates that the mesoporous of multilayer adsorption have occurred. For the N_2 adsorption-desorption curve of $178 \text{ }\mu\text{m}$ graphene aerogel, there is a smaller hysteresis loop in the middle-pressure zone and stronger adsorption and desorption in the high-pressure zone, which may result from the formation of larger pores in some lamellas (Figure 2(d)). Among the four samples, GA-11 has the largest specific surface area ($185.96 \text{ m}^2/\text{g}$), such a larger value is conducive to reduce the effective current density during lithium deposition.

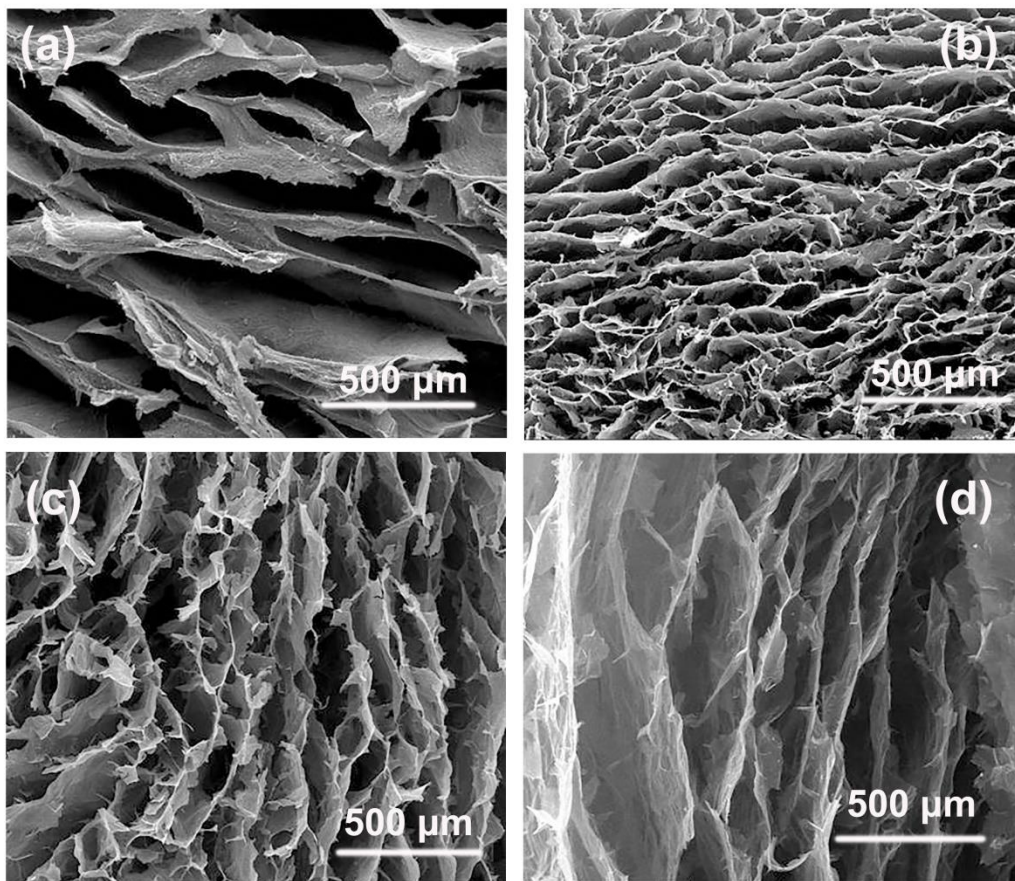


Figure 1. The SEM images of graphene aerogels prepared from natural graphite with different layer dimensions of (a) 3.4 μm , (b) 11 μm , (c) 44 μm and (d) 178 μm .

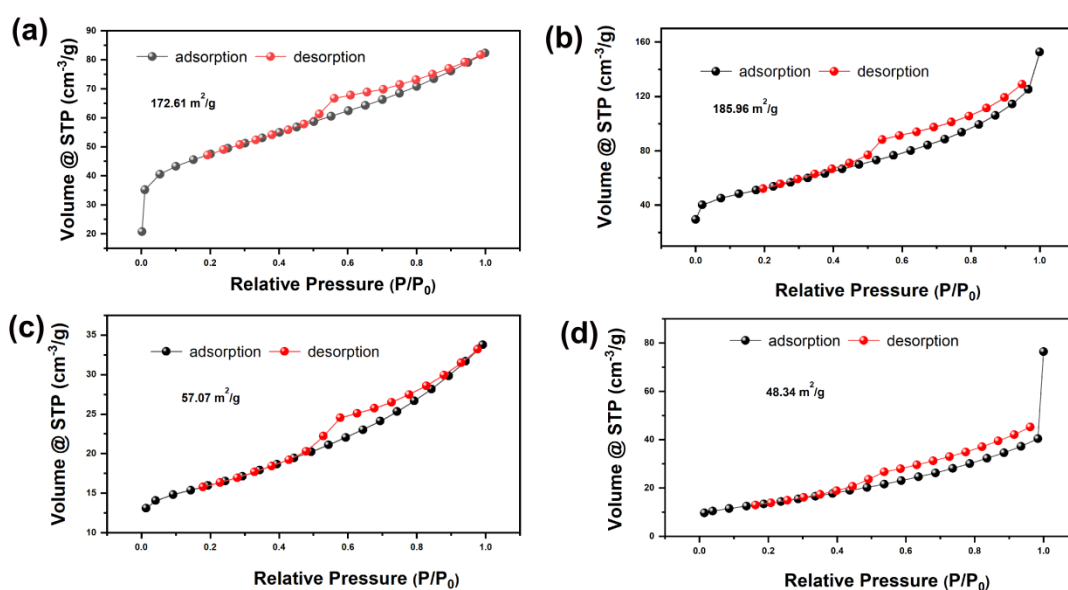


Figure 2. Nitrogen adsorption/desorption isotherms of graphene aerogels prepared from natural graphite with different layer dimensions of (a) 3.4 μm , (b) 11 μm , (c) 44 μm and (d) 178 μm .

In order to evaluate which graphene aerogel sample is the most ideal Li framework, the electrochemical performances of symmetrical cells were evaluated. In all GA/Li composite electrodes, the mass fraction of Li is as high as 90%. With the specific hierarchical porous structure and large specific surface area characteristic, the symmetrical GA-11/Li | GA-11/Li cell exhibits good stable cycling performance compared with that of lithium symmetrical cells in reported literature [13, 15]. At a current density of 2 mA cm^{-2} , the voltage-time graphs of symmetrical cells with different GA/Li and commercial Li foil electrodes are shown in Figure 3, the capacity is 2 mAh cm^{-2} . Among all the symmetrical cells, the symmetrical GA-11/Li | GA-11/Li cell exhibits the best electrochemical performance, it displays a relatively small and flat voltage hysteresis of 20 mV over 600 h. On the contrary, the commercial Li foil symmetrical cell reveals a larger overpotential of 43 mV and sharply increases to 500 mV within 210 h, owing to the continuously generated Li dendrites, the unstable solid electrolyte interface and continuous generation of dead Li.

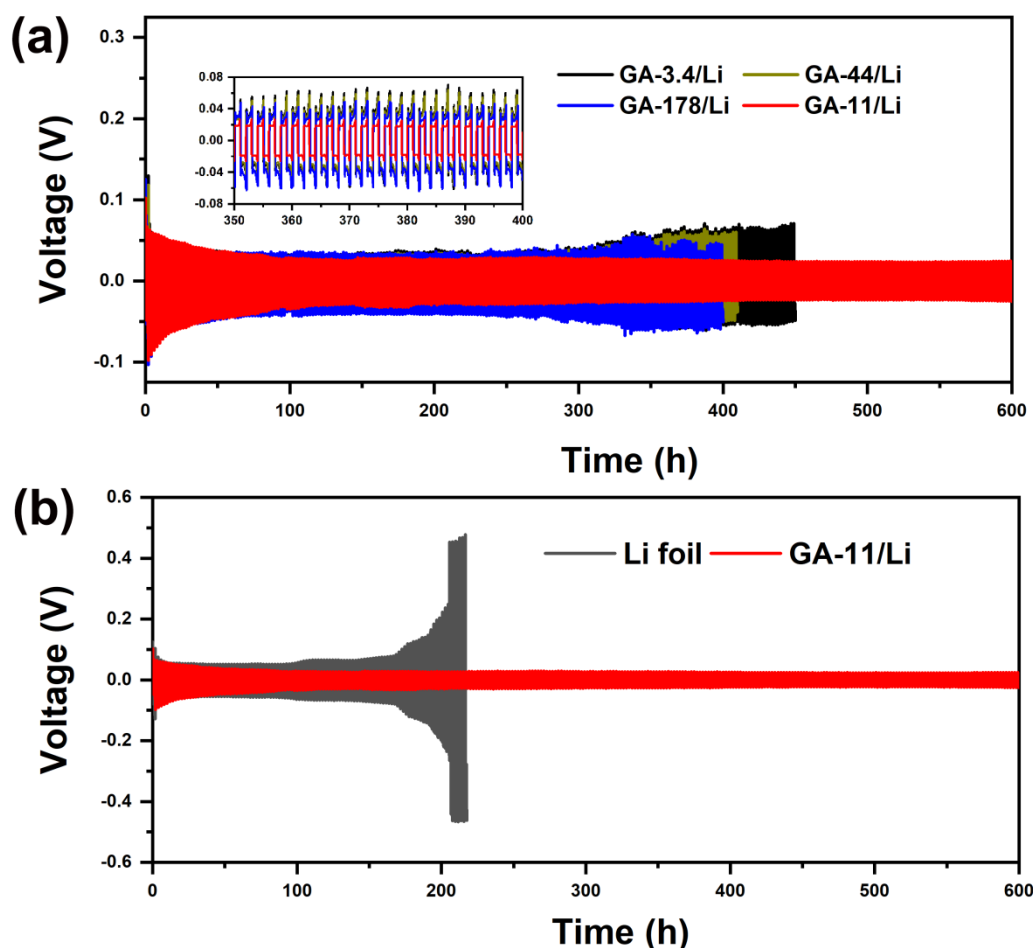


Figure 3. At 2 mA cm^{-2} , 2 mAh cm^{-2} , (a) Voltage profiles of symmetric cells with different GA/Li composite anodes, inset of (a) is the magnified stripping-plating profiles between 350 h and 400 h, (b) Voltage profiles of GA-11/Li | GA-11/Li and Li | Li foil symmetric cells.

Figure 4 shows the top view images of commercial Li foil and GA-11/Li electrodes with a capacity 1 mAh cm^{-2} after 20 stripping/plating cycles at a current density of 1 mA cm^{-2} . There are

numerous Li dendrite and mossy dead Li formation on the commercial lithium foil (Figure 4(a) and (b)). The lithium dendrites not only reduce the cycle life of the lithium metal battery, but also cause short circuits and even lead to fire accident. Encouragingly, the GA-11/Li electrode exhibits a totally different morphology (Figure 4(c) and (d)), the electrode surface is relatively smooth and compact with no obvious lithium dendrites and dead Li, which suggests that the graphene aerogel-11 as an unique lithium host material improves the stability of Li composite anode. After cycles, the relatively smooth surface of GA-11/Li electrode compared to the mossy commercial Li electrode originate from the following characteristics of GA-11: (1) graphene layers self-assemble to form an interconnected lightweight 3D graphene aerogel with a unique hierarchical porous structure and numerous open pore channels, which is beneficial to moderate the huge volume expansion in lithium plating/stripping cycles; (2) benefit from the large specific surface area and uniform distribution of Li^+ ions, lithium is flatly deposited on the GA-11 host and the nucleation and growth of Li dendrites are inhibited.

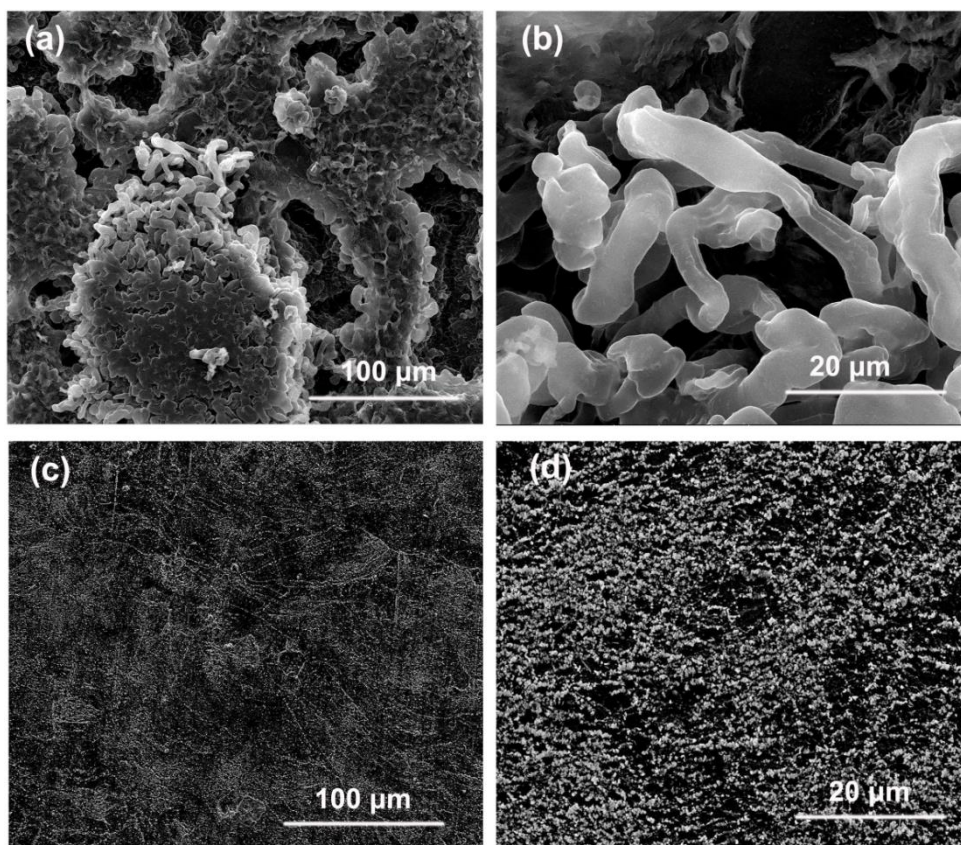


Figure 4. Top view SEM images of (a, b) commercial Li foil and (c, d) GA-11/Li after 20 stripping/plating cycles (1 mA cm^{-2} , 1 mAh cm^{-2}).

To investigate the potential application of the GA-11/Li anode, the electrochemical performance of Li-S full cells with GA-11/Li electrode as anode were investigated (Figure 5), the sulfur loadings are 9.4 mg cm^{-2} . The full cell with GA-11/Li anode (GA-11/Li | S full cell) delivers a stable cycle performance and high CE. The GA-11/Li | S full cell delivers a high primary areal capacity of 9.38 mAh cm^{-2} , and 5.5 mAh cm^{-2} capacity can be maintained after 78 cycles and no obvious internal short circuit during whole cycles.

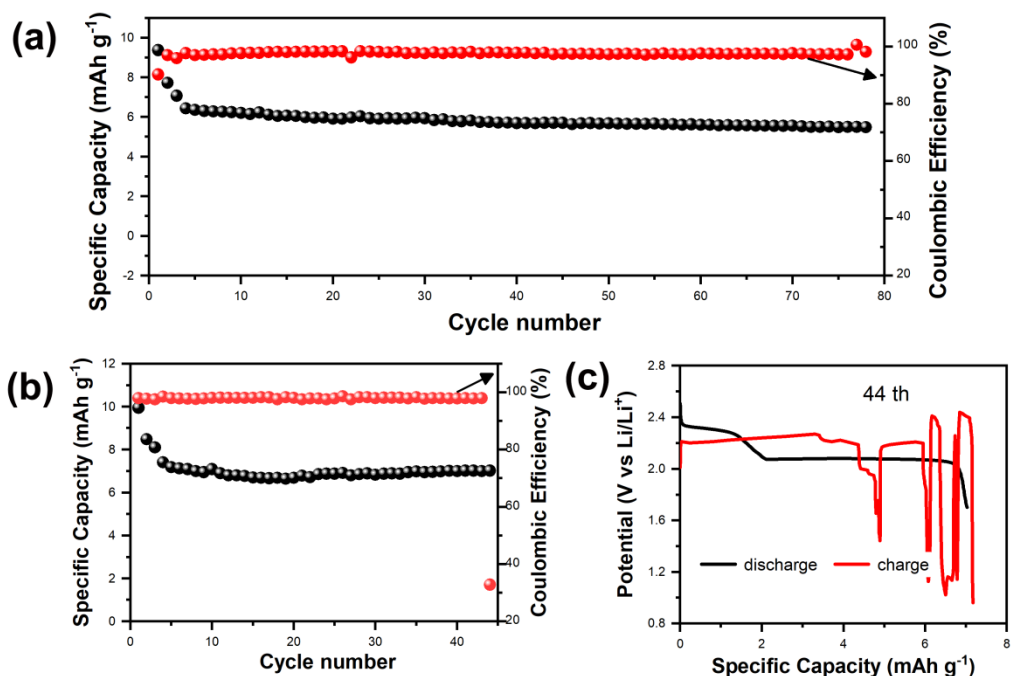


Figure 5. Capacity retention and coulombic efficiency of (a) GA-11/Li | S full cell and (b) Li | S full cell, (c) the 44th cycle galvanostatic discharge-charge profiles of Li | S full cell at 1 mA cm⁻² after three formation cycles at 0.5 mA cm⁻². The sulfur loadings of the two cells are as high as 9.4 mg cm⁻².

Table 1. Performance comparison of lithium-sulfur full cells assembled with different Li composite anodes, whose hosts are different carbon materials

Host materials in Li metal anodes	Li amount in composite Li anodes	Sulfur loading in S cathodes	Initial Capacity of Li-S full cell with different Li anodes	Cycle performance of Li-S full cell with different Li anodes	Ref.
Graphene aerege-11	90 wt%	9.4 mg/cm ²	9.38 mAh/cm ²	5.5 mAh/cm ² after 78 cycles	This work
Graphene aerogel	83.3 wt%	10 mg/cm ²	10.5 mAh/cm ²	5 mAh/cm ² after 50 cycles	[16]
Carbon fiber	53.2 wt%	1.7 mg/cm ²	3.25 mAh/cm ²	3.2 mAh/cm ² after 100 cycles	[22]
ZnO/carbon nanotubes	—	2.5 mg/cm ²	3.25 mAh/cm ²	1.73 mAh/cm ² after 100 cycles	[23]
Carbon fiber/Ag	40.7 wt%	1.7 mg/cm ²	1.89 mAh/cm ²	0.86 mAh/cm ² after 400 cycles	[24]
Multilayered graphene	—	—	6.2 mAh/cm ²	3.6 mAh/cm ² after 180 cycles	[25]

However, an internal short circuit and a sudden dropping of the charging voltage occur in the 44th cycle of Li | S, due to the continuous generation of Li dendrites. These results imply that abundant holes and large specific area of GA-11 are effective to moderate the volume changes during cycles and restrain the formation of Li dendrites. The properties comparison of lithium-sulfur full batteries assembled with different Li composite anodes, whose hosts are different carbon materials are shown in Table 1. By comparing the data in the table, the Li amount of GA-11/Li composite anode in this work reaches 90 wt% (Li amounts <70 wt% in most references), due to the ultra-low mass density (9 mg cm^{-3}) and porous structure of GA-11. The high Li amount enables the GA-11/Li composite deliver much higher energy density than reported Li composites. The initial areal capacity of GA-11/Li | S full cell is much higher than that of most of reported similar Li-S cells, while stable cycle performance is preserved. These results demonstrate that the graphene aerogel-11 is an ideal host material of lithium anode and GA-11/Li composite shows the potential in practical application.

4. CONCLUSIONS

In summary, a series of graphene aerogels have been prepared by a hydrothermal method, whose raw materials are natural graphite with different lateral dimensions (3.4 μm 、11 μm 、44 μm 、178 μm). All four graphene aerogels have interconnected 3D porous structures, large specific surface area and ultra-low density, which can migrate the volume change, inhibit Li dendrites and realize a high Li mass fraction (90 wt%). When GA-11 is used as host material for Li metal electrode, the cyclic stability of the GA-11/Li symmetrical cell is the most excellent. Under the condition of 2 mA cm^{-2} , 2 mAh cm^{-2} , the symmetrical GA-11/Li | GA-11/Li cell holds a stable polarization potential of 20 mV for 600 h. The GA-11/Li | S full cell with a high sulfur content of 9.4 mg cm^{-2} delivers a high initial specific discharge capacity of 9.38 mAh cm^{-2} and stable cycle stability.

ACKNOWLEDGEMENTS

This work was supported by National Natural Science Foundation of China (No.21965017), Chengdu Science and Technology office, the Western Young Scholars of the Chinese and Technology Innovation Seedling Project of Sichuan Province (No. 2020070).

References

1. D. Lin, Y. Liu, Y. Cui, *Nat. Nanotec.*, 12 (2017) 194.
2. J.M. Tarascon, M. Armand, *Nature*, 414 (2001) 359.
3. H. Ye, Z.J. Zheng, H.R. Yao, S.C. Liu, T.T. Zuo, X.W. Wu, Y.X. Yin, N.W. Li, J.J. Gu, F.F. Cao, Y.G. Guo, *Angew. Chem. Int. Ed.*, 58 (2019) 1094.
4. K. Pu, X. Qu, X. Zhang, J. Hu, C. Gu, Y. Wu, M. Gao, H. Pan, Y. Liu, *Adv. Sci.*, 6 (2019) 1901776.
5. S. Li, W. Zhang, Q. Wu, L. Fan, X. Wang, X. Wang, Z. Shen, Y. He, Y. Lu, *Angew. Chem. Int. Ed.*, 59 (2020) 2.
6. Y.L. Xiao, B. Han, Y. Zeng, S.S. Chi, X. Zeng, Z. Zheng, K. Xu, Y.H. Deng, *Adv. Energy Mater.*, 10 (2020) 1903937.
7. X. Zheng, Z. Gu, X. Liu, Z. Wang, J. Wen, X. Wu, W. Luo, Y. Huang, *Energy Environ. Sci.*, 13

- (2020) 1788.
8. J.S. Kim, D.W. Kim, H.T. Jung, J.W. Choi, *Chem. Mater.*, 27 (2015) 2780.
 9. C.P. Yang, Y.X. Yin, S.F. Zhang, N.W. Li, Y.G. Guo, *Nature. Com.*, 6 (2015) 8058.
 10. D. Lin, Y. Liu, Z. Liang, H.W. Lee, J. Sun, H. Wang, K. Yan, J. Xie, Y. Cui, *Nat. Nanotec.*, 11 (2016) 626.
 11. G. Huang, J. Han, F. Zhang, Z. Wang, H. Kashani, K. Watanabe, M. Chen, *Adv. Mater.*, 31 (2019) 1805334.
 12. R. Zhang, X. Chen, X. Shen, X.Q. Zhang, X.R. Chen, X.B. Cheng, C. Yan, C.Z. Zhao, Q. Zhang, *Joule*, 2 (2018) 764.
 13. Y. Zhang, B. Y. Liu, E. Hitz, W. Luo, Y.G. Yao, Y. Li, J.Q. Dai, C.J. Chen, Y.B. Wang, C.P. Yang, H.B. Li, L.B. Hu, *Nano Res*, 10 (2017) 1356.
 14. C. Cui, C. Yang, N. Eidson, J. Chen, F. Han, L. Chen, C. Luo, P.F. Wang, X. Fan, C. Wang, *Adv. Mater.*, 32 (2020) 1906427.
 15. L. Liu, Y.X. Yin, J.Y. Li, N.W. Li, X.X. Zeng, H. Ye, Y.G. Guo, L.J. Wan, *Joule*, 1 (2017) 563.
 16. W. Huang, Y. Yu, Z. Hou, Z. Liang, Y. Zheng, Z. Quan, Y.C. Lu, *Energy Storage Mater.*, 33 (2020) 329.
 17. Y. Yang, M. Zhao, H. Geng, Y. Zhang, Y. Fang, C. Li, J. Zhao, *Chem. Eur. J.*, 25 (2019) 5036.
 18. B. Yu, T. Tao, S. Mateti, S. Lu, Y. Chen, *Adv. Funct. Mater.*, 28 (2018) 1803023.
 19. Z.J. Wang, H. Gao, Q. Zhang, Y.Q. Liu, J. Chen, Z.P. Guo, *Small*, 15 (2019) 1803858.
 20. Q.Q. Zhang, X. Xu, D. Lin, W.L. Chen, G. Xiong, Y. Yu, T.S. Fisher, H. Li, *Adv. Mater.*, 28 (2016) 2229.
 21. T.Y. Yang, L. Li, F. Wu, R.J. Chen, *Adv. Funct. Mater.*, 30 (2020) 2002013.
 22. P. Shi, T. Li, R. Zhang, X. Shen, X.B. Cheng, R. Xu, J.Q. Huang, X.R. Chen, H. Liu, Q. Zhang, *Adv. Mater.*, 31 (2019) 1807131.
 23. H. Zhang, X.B. Liao, Y.P. Guan, Y. Xiang, M. Li, W.F. Zhang, X. Zhu, H. Ming, L. Lu, J. Qiu, Y. Huang, G. Cao, Y.S. Yang, L.Q. Mai, Y. Zhao, H. Zhang, *Nature. Com.*, 9 (2018) 3729.
 24. R. Zhang, X. Chen, X. Shen, X.Q. Zhang, X.R. Chen, X.B. Cheng, C. Yan, C.Z. Zhao, Q. Zhang, *Joule*, 2 (2018) 764.
 25. J.S. Kim, D.W. Kim, H.T. Jung, J.W. Choi, *Chem. Mater.*, 27 (2015) 2780.